Diffusion Tensor Tractography of Human Spinocerebellar, Cortico-Ponto-Cerebellar and Dentate-Rubro-Thalamo-Cortical Pathways

Khader M Hasan[1], Zafer Keser[2], Arash Kamali[3], Nuray Yozbatiran[2], and Gerard E Francisco[2]

[1]Diagnostic and Interventional Imaging, University of Texas Health Science Center, Houston, Texas, United States, [2]Physical Medicine and Rehabilitation, University of Texas Health Science Center and TIRR NeuroRecovery Research Center, Houston, Texas, United States, [3]Department of Diagnostic Radiology, Division of Neuroradiology, Johns Hopkins University, Maryland, United States

Introduction: The human cerebellum lies in the posterior fossa of the cranium with tentorium separating it from cerebrum. All input to and output from the cerebellum is by way of the three cerebellar peduncles. Most afferents into the cerebellum are via the inferior and middle cerebellar peduncles and all output from the cerebellum is via the superior cerebellar peduncle. The cerebellar connections are functionally divided into the vestibulocerebellar, spinocerebellar and cerebrocerebellar connections. These three components make it easier to understand the complex pathways connecting cerebellum to extra-cerebellar structures (1). *Spinocerebellar (SC)* pathways project from spinal cord to cerebellum and play role in relaying non-conscious proprioceptive/kinesthetic information from muscle spindles and tendons non-conscious cutaneous feedback (e.g. pressure, touch and pain). Vestibulocerebellar connections are mainly from brainstem structures and maintain balance and equilibrium of the body (2). Cerebrocerebellar connections are composed of feed forward and feedback connections between cerebrum and cerebellum and considered as a loop (3). *Corticopontocerebellar (CPC)* pathways of cortical origin and d*entate-rubro-thalamo-cortical (DRTC)* pathway of cerebellar origin are responsible for fine-tuning the execution of voluntary movement, high order visual and auditory functions motor planning and high-order cognitive functions (4). In this study, we demonstrate the feasibility of *in vivo* delineation and 3D reconstruction of the main cerebellar pathways using high resolution diffusion tensor imaging (DTI) data on 3.0 T in a systematic way. We also identified and quantified bilaterally each tract volume and its corresponding DTI scalar metrics.

Methods: *Subjects*: Ten healthy subjects (age range 20-51 years) were studied and written informed consent was obtained from all subjects. *MRI Data Acquisition*: Data were acquired using a Philips 3.0 T Intera system using a SENSE receive head coil. The MRI protocol included conventional MRI (dual echo FSE, phase-sensitive, FLAIR & 3DT1-weighted anatomical). Diffusion-weighted image (DWI) data were acquired axially from the same graphically prescribed conventional MRI volumes using a single-shot multi-slice 2-D spin-echo diffusion sensitized and fat-suppressed echo planar imaging (EPI) sequence, with the balanced and alternating polarity *Icosa21* tensor encoding scheme (5,6). The b-factor = 1000 sec mm^{-2}, T_R/T_E = 9000/65 msec, FOV = 256 mm x 256 mm and slice thickness / gap/ #slices = 2 mm / 0 mm / 70. The EPI phase encoding used a SENSE k-space undersampling factor of two, with an effective k-space matrix of 112x112 and an image matrix after zero-filling of 256x256. The constructed image spatial resolution for DTI data was ~ 1 mm x 1 mm x 2 mm.

Tracts N=10	Tract Vol (mL = cm*cm*cm)	FA (μ ± σ)	MD (x10-3 mm*mm /sec)	RD (x10-3 mm*mm/ sec
R-SC	1.96±0.90	0.48±0.02	0.72±0.03	0.51±0.02
L-SC	1.73±0.57	0.47±0.02	0.73±0.04	0.53±0.03
p (R vs. L)	0.26	0.41	0.58	0.25
R-DRTC	2.69±0.71	0.55±0.02	0.74±0.02	0.47±0.02
L-DRTC	3.44±1.44	0.56±0.02	0.73±0.02	0.46±0.02
p (R vs. L)	0.32	0.42	0.06	0.16
R-FPC	4.71±1.51	0.56±0.01	0.72±0.05	0.46±0.04
L-FPC	5.29±2.08	0.56±0.02	0.72±0.03	0.47±0.03
p (R vs. L)	0.49	1.00	0.74	0.68
R-PPC	2.27±1.35	0.54±0.03	0.73±0.02	0.48±0.03
L-PPC	2.51±2.16	0.52±0.03	0.74±0.03	0.50±0.04
p (R vs. L)	0.74	0.08	0.22	0.15
R-TPC	0.90±0.26	0.51±0.03	0.74±0.03	0.50±0.04
L-TPC	1.10±0.97	0.53±0.03	0.79±0.04	0.53±0.03
p (R vs. L)	0.46	0.20	**0.02**	0.13
R-OPC	1.38±0.64	0.56±0.04	0.71±0.02	0.46±0.03
L-OPC	2.62±1.13	0.55±0.02	0.74±0.02	0.47±0.02
p(R vs. L)	**0.01**	0.85	**0.01**	0.14

Anatomical Landmarks: **SC pathways** originate from spinal cord mainly passes through the inferior cerebellar peduncle (ICP) to enter the cerebellum. **CPC pathways** arising from different parts of the cortex pass through middle cerebellar peduncle (MCP) and reach to the cerebellar hemisphere. **DRTC pathways** emerging from dentate nuclei, together with interposed nuclei, traverse superior cerebellar peduncle (SCP) reach to red nucleus or directly to of thalamus then to cortex (1)

Fiber Tracking. We have used a brute force and multiple ROI tracking method and the FACT algorithm (8, 9) (DTIStudio) to reconstruct *spinocerebellar (SC), DRTC, fronto-ponto-cerebellar (FPC), parieto-ponto-cerebellar (PPC), temporo-ponto-cerebellar (TPC) and occipito-ponto-cerebellar (OCP)* pathways with a fractional anisotropy (FA) threshold of 0.15 and angle threshold of 70 degrees. Statistical comparisons were made using analysis-of-variance (student paired t-test).

Results: Figure 1 illustrates the construction of Spinocerebellar (SC) (a), DRTC (b), FPC(c)PPC(d), TPC(e), OPC(f) and fusion with the T1w data. **Figure 2.** Illustrates the ROI placements. **Table 1** below provides a summary of the mean and standard deviations of the tract volumes and corresponding FA and means diffusivity (MD) values of the bilateral SC, DRTC, FPC, PPC, TPC and OPC fiber tracts on the ten subjects. Note that mean diffusivities of Left TPC and OPC are significantly higher than right ones. Left OPC has significantly higher volume than right OPC.

Discussion and Conclusions: In this work, we have demonstrated that main cerebellar pathways could be delineated and quantified using 2 mm DTI data sets. Although these tracts have been described previously (10, 11, 12), a clear deterministic tractography protocol to reconstruct all these tracts and their corresponding DTI attributes has not been reported. On the other hand, while the cerebellum's role in motor function is well-known, the nature of its concurrent role in high-order cognitive and emotional functions has received increased interest recently (3). We believe that revealing the connections of cerebellum with extracerebellar structures is a crucial step in understanding underestimated roles of cerebellum. Extension of this preliminary work will be the application of the methods to the patient populations such as autism, stroke, traumatic brain injury, spinal cord injury and multiple sclerosis.

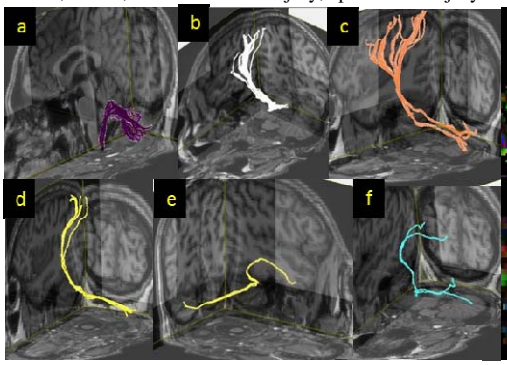

Figure 1. 3D views of the SC (a), DRTC (b), FPC (c) ,PPC (d), TPC (e) and OCP (f) pathways.

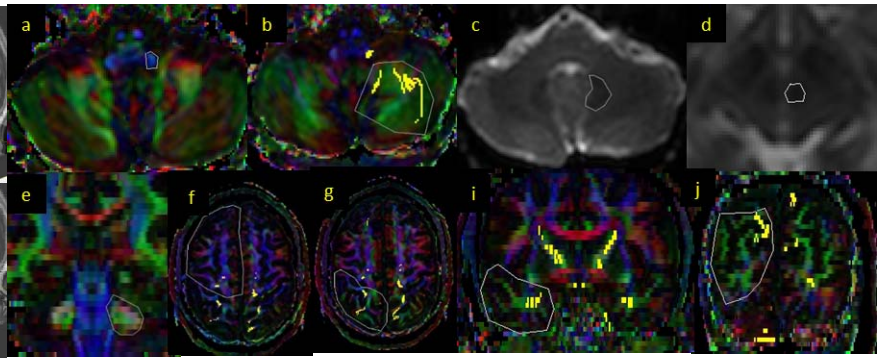

Figure 2 .ROI is seeded in ICP (a) and Cerebellar Hemisphere (b) for SC Tract and in Dentate (c) and Red Nuclei (d) for DRTC. Coronal section of MCP being the first ROI for CPC pathways(e), axial section of frontal lobe (f) for FPC, axial section of parietal lobe (g) for PPC coronal section of temporal lobe (i) for TPC and coronal section of occipital lobe (j) for OPC are chosen as second ROI. DTI color coded (a,b and e-j) and b0 (c and d) maps are used for ROI determination.

References

1. Mendoza J et al. Clinical neuroanatomy Springer; 1st Ed 2007.
2. Snell, R. Clinical neuroanatomy. Seventh ed. LWW; 2009.
3. Koziol LF et al. The Cerebellum. 2013;13:151-177.
4. Blumenfield, H. Neuroanatomy through clinical cases, Sinauer Ass., Inc.; 2nd ed;2011.
5. Hasan KM et al. Magn Reson Med. 2009:59:7-13.
6. Hasan KM et al. Magn Reson Med. 2009;23:631-6.
7. Mori S, et al. Magn Reson Med. 2002;47:215-223.
8. Alexander AL, et al. Magn Reson Med. 2001;45:770-780.
9. Mori S and van Zijl PC. NMR Biomed. 2002; 15:468-480.
10.Kamali A Jour of Mag Resonan Imaging. 2010;32:809-817.
11. Catani M et al. NeuroImage. 2008;41:1184-1191.
12. Marek M et al. Journal of Neurology. 2014 Doi=10.1007/s00415-014-